Lipari, G., & Szabo, A. (1982a) *J. Am. Chem. Soc. 104*, 4546.
Lipari, G., & Szabo, A. (1982b) *J. Am. Chem. Soc. 104*, 4559.
Loll, P. G., & Lattman, E. E. (1989) *Proteins: Struct., Funct., Genet. 5*, 1983.
Marion, D., & Wüthrich, K. (1983) *Biochem. Biophys. Res. Commun. 113*, 967.
Markley, J. L., Jorsley, W. J., & Klein, M. P. (1971) *J. Chem. Phys. 55*, 3604.
McCain, D. C., Ulrich, E. L., & Markley, J. L. (1988) *J. Magn. Reson. 80*, 296.
Meiboom, S., & Gill, D. (1958) *Rev. Sci. Instrum. 29*, 688.
Neri, D., Szyperski, T., Otting, G., Seen, H., & Wüthrich, K. (1989) *Biochemistry 28*, 7510.
Nirmala, N. R., & Wagner, G. (1988) *J. Am. Chem. Soc. 110*, 7557.
Nirmala, N. R., & Wagner, G. (1989) *J. Magn. Reson. 82*, 659.
Palmer, A. G., III, Rance, M., & Wright, P. E. (1991a) *J. Am. Chem. Soc. 113*, 4371.
Palmer, A. G., III, Wright, P. E., & Rance, M. (1991b) *Chem. Phys. Lett. 185*, 41.
Press, W. H., Flannery, B. P., Teukolsky, S. A., & Vetterling, W. T. (1988) in *Numerical Recipes in C*, pp 317–323, Cambridge University Press, Cambridge.
Richarz, R., Nagayama, K., & Wüthrich, K. (1980) *Biochemistry 19*, 5189.
Shaka, A. J., Keeler, J., & Freeman, R. (1983) *J. Magn. Reson. 53*, 313.
Sklenar, V., Torchia, D. A., & Bax, A. (1987) *J. Magn. Reson. 73*, 375.
Sparks, S. W., Cole, H. B. R., Torchia, D. A., & Young, P. E. (1989) *Chem. Scr. 29A*, 31.
Spiess, H. W. (1978) *NMR: Basic Princ. Prog. 15*, 55.
Spiess, H. W., Schweitzer, D., & Haeberlen, U. (1973) *J. Magn. Reson. 9*, 444.
Torchia, D. A., Sparks, S. W., & Bax, A. (1989a) *Biochemistry 28*, 5509.
Torchia, D. A., Sparks, S. W., Young, P. E., & Bax, A. (1989b) *J. Am. Chem. Soc. 111*, 8315.
Wang, J., LeMaster, D. M., & Markley, J. M. (1990a) *Biochemistry 29*, 88.
Wang, J., Hinck, A. P., Loh, S. N., & Markley, J. M. (1990b) *Biochemistry 29*, 4242.
Werbelow, L. G., & Grant, D. M. (1977) *Adv. Magn. Reson. 9*, 189.
Wittebort, R. J., Rothgeb, T. M., Szabo, A., & Gurd, F. R. N. (1979) *Proc. Natl. Acad. Sci. U.S.A. 76*, 1059.
Woessner, D. E. (1962) *J. Chem. Phys. 36*, 1.

^{1}H NMR and NOE Studies of the Purple Acid Phosphatases from Porcine Uterus and Bovine Spleen†

Zhigang Wang, Li-June Ming, and Lawrence Que, Jr.*
Department of Chemistry, University of Minnesota, Minneapolis, Minnesota 55455
John B. Vincent, Michael W. Crowder, and Bruce A. Averill
Department of Chemistry, University of Virginia, Charlottesville, Virginia 22901
Received January 23, 1992; Revised Manuscript Received April 2, 1992

ABSTRACT: The diiron active sites of the purple acid phosphatases from porcine uterus (also called uteroferrin, Uf) and bovine spleen (BSPAP) and their complexes with tungstate are compared by ^{1}H NMR and NOE techniques. The paramagnetically shifted features of the ^{1}H NMR spectrum of reduced BSPAP are similar to those of reduced Uf, while the spectra of the tungstate complexes are almost identical. These observations suggest that the two active sites are quite similar, in agreement with the >90% sequence homology found in the two enzymes. Nuclear Overhauser effect (NOE) experiments on the His N–H resonances show that the Fe(III)–His residue is N_ϵ-coordinated, while the Fe(II)–His is H_δ-coordinated in both enzymes. On the basis of the above NMR and NOE results, our previously proposed model for the dinuclear iron active site of Uf [Scarrow, R. C., Pyrz, J. W., & Que, L., Jr. (1990) *J. Am. Chem. Soc. 112*, 657–665] is corroborated, refined, and found to represent the diiron center of BSPAP as well.

Purple acid phosphatases (PAP's), a class of enzymes isolated from a wide variety of animal and plant sources, catalyze the hydrolysis of certain phosphate esters, including nucleotide di- and triphosphates and aryl phosphates in vitro (Antanaitis & Aisen, 1983; Doi et al., 1988; Vincent & Averill, 1990). The most throughly studied PAPs are the mammalian enzymes from porcine uterus (also called uteroferrin, Uf) (Antanaitis et al., 1980, 1983) and bovine spleen (BSPAP) (Davis & Averill, 1982; Averill et al., 1987), which are glycoproteins with molecular mass of 35–40 kDa (Antanaitis & Aisen, 1983; Doi et al., 1988; Vincent & Averill, 1990). Uf consists of a single polypeptide chain, while BSPAP has two polypeptide chains which possibly arise from proteolysis during purification. The amino acid sequences of Uf and BSPAP exhibit greater than 90% homology (Hunt et al., 1987; Ketcham et al., 1989). The similarities in sequence and substrate specificity suggest that these enzymes may perform similar functions in vivo, despite the fact that Uf is an extracellular enzyme in porcine uterus while BSPAP is localized in bovine spleen cells.

†This work was supported by grants from the National Science Foundation (DMB-9104669 to L.Q.) and the National Institutes of Health (GM 32117 to B.A.A.). J.B.V. acknowledges the support of an NIH postdoctoral fellowship (GM 13500).

0006-2960/92/0431-5263$03.00/0

One important structural feature of the mammalian PAP's is the dinuclear iron center which, along with a nearby His residue that can be phosphorylated during the catalytic cycle, comprises the active site (Vincent et al., 1991a). This diiron center can exist in two interconvertible oxidation states. The reduced Fe(III)Fe(II) state is catalytically active and exhibits a rhombic EPR spectrum with g values at 1.94, 1.76, and 1.56 (Schlosnagle et al., 1976; Campbell et al., 1978; Antanaitis et al., 1980, 1983; Averill et al., 1987), typical of mixed-valence diiron centers (Que & True, 1990), while the oxidized Fe(II)Fe(III) state is EPR-silent and exhibits some catalytic activity toward phosphate ester hydrolysis (Dietrich et al., 1991). The purple color associated with PAP's results from a tyrosinate-to-Fe(III) charge-transfer transition, as demonstrated by resonance Raman spectroscopy (Averill et al., 1987; Gaber et al., 1979; Antanaitis & Aisen, 1982). The lack of any change in the extinction coefficient upon oxidation of the reduced enzyme suggests that tyrosinate is bound as a ligand only to the Fe(III) site in the reduced enzyme. Quantitative EPR (Antanaitis et al., 1983; Averill et al., 1987) and magnetic susceptibility measurements (Mockler et al., 1983; Sinn et al., 1983; Averill et al., 1987; Day et al., 1988) indicate that the dinuclear iron centers of mammalian PAP's are antiferromagnetically coupled, resulting in $S = 0$ and $S = {}^1/_2$ ground states in the oxidized and reduced forms, respectively. This antiferromagnetically coupled diiron center is responsible for the unusual optical, magnetic, and enzymatic properties of the enzymes.

^{1}H NMR spectroscopy has proved very useful for probing the metal environments of many paramagnetic metalloproteins via the isotropically shifted resonances arising from the nuclei in close proximity of the metal (Bertini & Luchinat, 1986). We have previously reported a structural model for the dinuclear iron center of Uf based on our ^{1}H NMR studies of reduced Uf and its oxoanion complexes (Lauffer et al., 1983; Scarrow et al., 1990). Until recently, the diiron centers of Uf and BSPAP appeared different, particularly with respect to their chemistry with anions. With the preparation of the high-salt-stabilized form of BSPAP, the behavior of the two enzymes has become quite analogous (Vincent et al., 1991b). In this work, comparative NMR studies on reduced Uf (Uf_r) and reduced BSPAP ($BSPAP_r$) are reported. Using the nuclear Overhauser effect (NOE), we unambiguously assign many of the resonances arising from the coordinated ligands in the diiron center. The new data not only give us strong evidence for the similarities between the diiron centers of Uf and BSPAP but also allow us to corroborate and refine our proposed model for the PAP diiron active site.

Experimental Procedures

Protein Samples. Uteroferrin was isolated and purified from the uteri of gilts treated with β-estradiol 17-valerate according to the literature procedures (Basha et al., 1980; Pyrz et al., 1986) with slight modification. Bovine spleen purple acid phosphatase was isolated and purified as previously described (Vincent et al., 1991b). The high-salt-stabilized form of BSPAP was used to perform the NMR studies. The purity of the enzymes was judged by their optical spectra ($A_{280}/A_{\lambda_{max}} < 14$), enzymatic activity, and polyacrylamide gel electrophoresis. Enzymatic activity was determined as previously described with 10 mM p-nitrophenyl phosphate as substrate in 0.1 M MES buffer at pH 4.9 for Uf (Schlosnagle et al., 1976) and pH 6.0 for BSPAP (Campbell et al., 1978). The specific activity for Uf was larger than 300 mmol/mg·min after treatment with β-mercaptoethanol and catalytic amounts of $Fe(NH_4)_2(SO_4)_2$, while the specific activity for BSPAP was 1200 mmol/mg·min after treatment with ascorbate and catalytic amounts of $Fe(NH_4)_2(SO_4)_2$.

The tungstate complexes of Uf and BSPAP were prepared by addition of a freshly made solution of 1.1 molar equiv of Na_2WO_4 to dilute solution of Uf or BSPAP, followed by enzyme concentration and degassing.

NMR Spectroscopy. ^{1}H NMR spectra and NOE difference spectra were taken at 30 °C on an IBM NR-300 spectrometer operating at 300 MHz. A total of 16K data points were collected over an 80-kHz bandwidth. Signal-to-noise ratios were improved by using a line-broadening factor of 30 Hz in the Fourier transformation. Samples in both H_2O (100 mM acetate, pH 4.9) and D_2O (100 mM acetate, pD 4.9) buffer were studied. The NMR samples in H_2O buffer were prepared by concentrating the enzyme solution in a Centricon-10 microconcentrator (Amicon Corp., Danvers, MA), and those in D_2O buffer were obtained by repeatedly concentrating in a Centricon-10 microconcentrator and diluting with D_2O buffer. The concentration of the Uf samples was about 5 mM, whereas the concentration of the BSPAP samples was about 1 mM. The BSPAP samples could not be further concentrated due to protein precipitation. For the ^{1}H NMR experiments, 20 000 transients for Uf samples and 100 000 transients for BSPAP samples were collected. The "modified DEFT" technique (Hochmann & Kellerhals, 1980), which uses a pulse sequence of $90°-\tau-180°-\tau-90°$ to suppress the H_2O signal, was employed to observe the ^{1}H NMR resonances of samples in H_2O. The recycle time for taking the NMR spectra was set at 200 ms, during which time all the isotropically shifted resonances had recovered to their equilibrium states. For the NOE measurements, steady-state NOE's were obtained by using irradiation power of $\leq$0.2 W and 30–60-ms irradiation time in all the experiments. The NOE difference FID was obtained by computer addition and subtraction of the FID's with the decoupler pulse set alternately on the signal of interest and a reference position every 200 scans until 120 000–200 000 transients were collected. The "super WEFT" technique (Inubushi & Becker, 1983) was chosen to supress the H_2O signal for the samples in H_2O buffer. Chemical shift values are reported relative to the H_2O or HOD resonance at 4.8 ppm with positive values indicating downfield shifts.

Results

^{1}H NMR Studies. Catalytically active mammalian PAP's contain an antiferromagnetically coupled dinuclear Fe(III)-Fe(II) center, which gives rise to paramagnetically shifted NMR resonances from protons on the ligands coordinated to their irons. Well-resolved isotropically shifted ^{1}H NMR features are observed due to the favorable electron spin–lattice relaxation time of the diiron center (Scarrow et al., 1990). On the basis of such studies, an active site structure for Uf has been previously proposed (Scarrow et al., 1990). Since there is strong evidence from other methods such as EPR and resonance Raman spectroscopies (Antanaitis & Aisen, 1983; Doi et al., 1988; Vincent & Averill, 1990) of a similarity in active site for Uf and BSPAP, we have compared the ^{1}H NMR spectrum of reduced BSPAP with that of Uf (Table I).

The paramagnetically shifted ^{1}H NMR spectra of reduced BSPAP in H_2O and D_2O are compared to that of reduced Uf in Figure 1. Overall, the ^{1}H NMR spectrum of $BSPAP_r$ is similar to that of Uf_r. On the basis of the integration of the peaks, both enzymes have the same number of protons in the $\delta > 27$ ppm region (downfield), though several of the signals overlap in the $BSPAP_r$ case. Signals a–h represent one proton each in the Uf_r spectrum (Scarrow et al., 1990), whereas for $BSPAP_r$ in H_2O the signals at 83.2 and 30.0 ppm correspond

Table I: NMR Chemical Shifts (ppm) of Uf_r, $BSPAP_r$, Uf_r–WO_4, and $BSPAP_r$–WO_4 at 30 °C[a]

peak	assignment	Uf_r	$BSPAP_r$	Uf_r–WO_4	$BSPAP_r$–WO_4
a	Fe^{III}–Tyr-$C_\beta H$	86.6	69.5	112.7	115.8
b (ex)	Fe^{III}–His-$N_\delta H$	88.4	83.2	88.3	89.2
c	Fe^{III}–Tyr-$C_\delta H$	70.0	69.5	72.1	73.4
d	Fe^{III}–Tyr-$C_\delta H$	62.4	69.5	72.1	73.4
e (ex)	Fe^{II}–His-$N_\epsilon H$	44.0	39.9	54.5	54.5
f	?	43.5	39.9	46.4	43.8
g	Fe^{II}–His-$C_\delta H$	43.5	39.9	44.2	47.0
h	?	29.5	30.0	28.1	28.3
i	Fe^{III}–His-$C\beta H$	23.4	24.0	23.7	25.1
j	Fe^{III}–Tyr-$C_\beta H$	15.1	n.o.	n.o.	12.0

[a] All samples were in 100 mM acetate buffer at pH 4.9 with 1 mM (BSPAP) or 5 mM (Uf) protein.

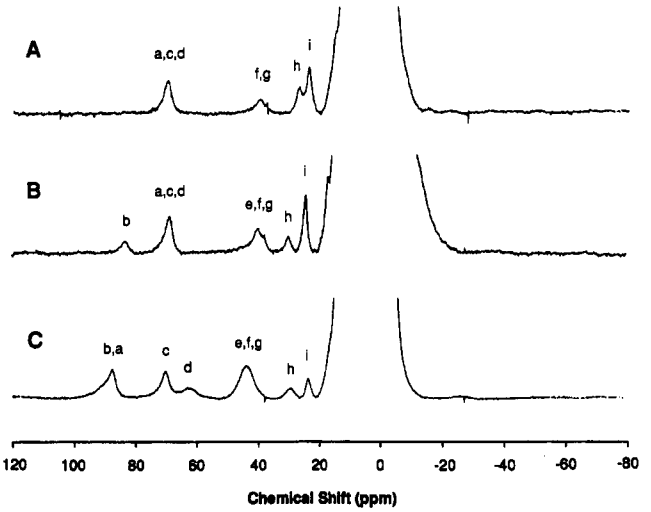

FIGURE 1: Proton NMR spectra of reduced BSPAP in D_2O buffer (A) and H_2O buffer (B) and reduced Uf in H_2O buffer (C) at 300 MHz and 30 °C in 100 mM acetate buffer at pH (pD) 4.9. The "modified DEFT" technique was used to suppress the water signal.

to one proton each and the signals at 69.5 and 39.9 ppm correspond to three protons each. However, the integration of the 24.0 ppm signal in the $BSPAP_r$ spectrum corresponds to three protons whereas its counterpart in the Uf_r spectrum (signal i) represents only one proton. The $BSPAP_r$ spectrum in D_2O buffer only gives four signals in the downfield region; the 83.2 ppm signal disappears, and the integration of the 39.9 ppm signal diminishes to two protons. The other two signals remain same. Therefore, like Uf_r, $BSPAP_r$ has two water-exchangeable signals in the downfield region, one at 83.2 ppm and the other at 39.9 ppm, consistent with N–H resonances on the His residues bound to Fe(III) and Fe(II), respectively. Several of the remaining resonances in the $BSPAP_r$ spectrum must arise from the tyrosine (peaks a, c, d, j, and y in Uf_r) whose presence is established by resonance Raman data (Averill et al., 1987; Gaber et al., 1979; Antanaitis & Aisen, 1982). Peak a, which is found at ca. 90 ppm in reduced Uf_r, must appear in a different region in the $BSPAP_r$ spectrum; on the basis of the effect of tungstate binding and the NOE results (vide infra), peak a has been assigned to one of the tyrosine β-CH_2 protons whose isotropic shift depends on the dihedral angle of the C–H bond and the C_γ p orbital (Scarrow et al., 1990). The different shifts for peak a in Uf_r and $BSPAP_r$ suggest that the conformations of the coordinated Tyr in the two enzymes are not identical. Upfield features found for Uf_r at −24.5 ppm (signal x) and −68 ppm (signal y) (Scarrow et al., 1990) are not observed in the spectrum of $BSPAP_r$, very likely due to their broadness.

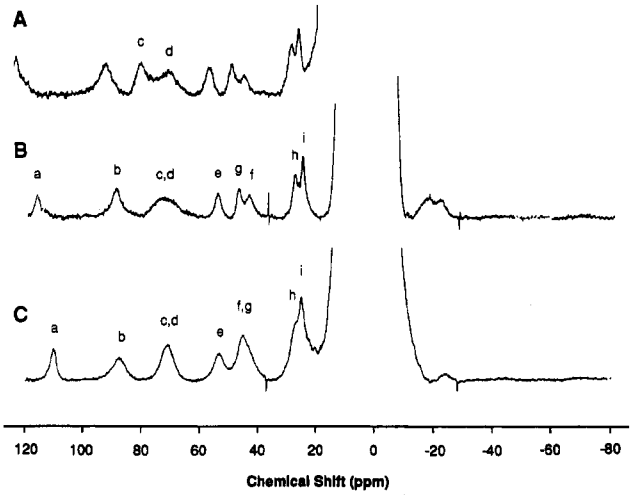

FIGURE 2: Proton NMR spectra of $BSPAP_r$–WO_4 in H_2O buffer (A, 15 °C; B, 30 °C) and Uf_r–WO_4 in H_2O buffer (C, 30 °C) at 300 MHz in 100 mM acetate buffer at pH 4.9. The "modified DEFT" technique was used to suppress the water signal.

The binding of tungstate causes almost all the overlapped signals in the spectrum of the native $BSPAP_r$ to become well resolved (Figure 2), revealing features that match quite well with those of Uf_r–WO_4. The three-proton signal at 69.5 ppm resolves at 15 °C into three signals at 123.1, 92.5, and 70.8 ppm. The latter two begin to coalesce at 30 °C into a broad feature at 73.4 ppm and are thus associated with the tyrosine C_δ–H's in intermediate exchange due to ring flipping (Lauffer et al., 1983). These three signals correspond to the signals a, c, and d in Uf_r–WO_4 (Figure 2) (Scarrow et al., 1990). The 83.2 ppm water-exchangeable signal moves downfield to 89.2 ppm when tungstate binds and corresponds to signal b in the Uf_r–WO_4 spectrum. Furthermore, the 39.9 ppm signal in BSPAP spectrum which represents 3 H's becomes three signals with chemical shifts at 43.8, 47.0, and 54.5 ppm (30 °C) upon tungstate binding, corresponding to signals e, f, and g of Uf_r–WO_4. The 54.5 ppm signal is water exchangeable and is analogous to peak e in Uf_r–WO_4. The 24.0 and 30.0 ppm signals which correspond to signal h and i in the Uf_r case are not affected significantly by tungstate binding except that they move closer to each other. There are two upfield signals in the $BSPAP_r$–WO_4 spectrum at −23 and −19 ppm, one of which may correspond to the −23.7 ppm upfield signal in the Uf_r–WO_4 case, but these can not be assigned at present. Overall, the ^1H NMR spectrum of $BSPAP_r$–WO_4 complex shares great similarities with that of Uf_r–WO_4.

NOE Measurements. Paramagnetic species have large nuclear relaxation rates, ρ_i, which can make NOE somewhat difficult to observe, as illustrated in

$$\eta_{ij}(t) = (\sigma_{ij}/\rho_i)[1 - \exp(-\rho_i t)] \quad (1)$$

where η_{ij} is the NOE on signal i when signal j is saturated for a period of time t (i.e., the fraction change in intensity of signal i when signal j is saturated) and $\sigma_{ij} = -h^2\gamma^4\tau_c/10r_{ij}^6$ is the cross-relaxation between i and j with τ_c being the rotational correlation time of the molecule and r_{ij} being the distance between nuclei i and j. However, when σ_{ij} is large enough to compensate for the large ρ_i, i.e., τ_c/r_{ij}^6 is very large, significant NOE can be observed. Therefore, NOE can be used to identify pairs of nuclei which are in close proximity of each other in paramagnetic molecules. We thus performed the NOE measurements on most of the downfield signals (Table II).

Figure 3 shows the NOE difference spectra of reduced Uf in D_2O buffer when signals a, c, d, h and i in the downfield

Table II: NOE Results on Uteroferin at 30 °C with 50-ms Irradiation Time

peak irradiated	T_1 (ms)	NOE peak	NOE magnitude
a	19.5	j	strong
		c	weak
		d	weak
c	7.7	a	weak
		j	weak
d	7.3	a	weak
		j	weak
b[a]	7.7	i	weak
e[a]	13.3	g	weak

[a] Results from the Uf_r–WO_4 complex.

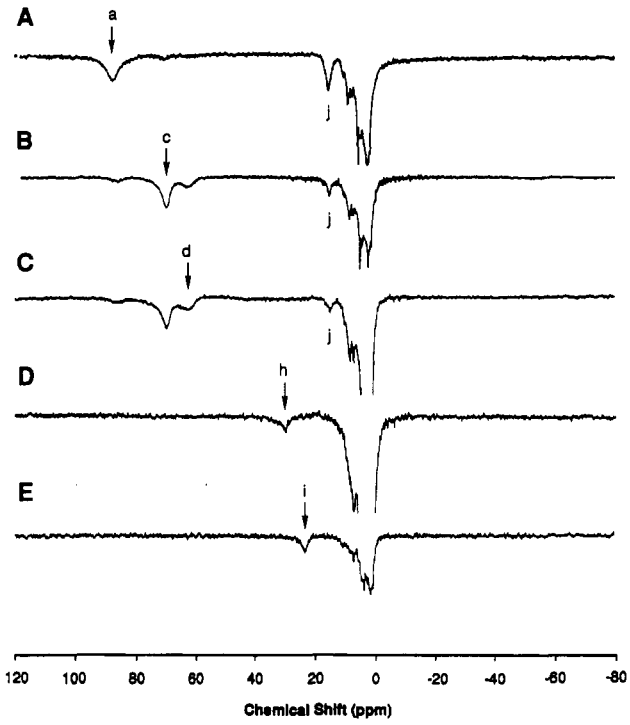

FIGURE 3: NOE difference spectra of reduced Uf in D_2O buffer at 300 MHz and 30 °C in 100 mM acetate buffer at pD 4.9. Irradiation signal and time: (A) signal a for 50 ms; (B) signal c for 50 ms; (C) signal d for 50 ms; (D) signal h for 30 ms; (E) signal i for 30 ms.

region are irradiated. When signal a is saturated, a significant NOE is observed on signal j, and weaker NOE's are found for signals c and d. These results suggest that H_a and H_j are in close proximity to each other with H_c and H_d being somewhat more distant. When either signal c or d is saturated, NOE's on signal a and j are observed. These observations confirm the previous assignment of the NMR signals to protons on the Fe(III)-coordinated tyrosine residue, i.e., a and j to the β-CH_2 protons and c and d to the Tyr C_δ-H protons, made on the basis of chemical shift assignments (Scarrow et al., 1990).

Irradiation of signals h and i does not reveal NOE's on any other signals; more importantly, there is no NOE correlation between signals h and i. This means H_h and H_i can not be the β-CH_2 protons of the histidine that coordinates to the Fe(III) site, as earlier suggested (Scarrow et al., 1990).

NOE studies on the solvent-exchangeable signals b and e were not carried out for native enzymes, since these two signals are not well separated from adjacent signals a, f, and g. The superior resolution of the signals in Uf_r–WO_4 allowed the NOE measurement to be performed on the solvent-exchangeable signals (Figure 4).

When signal b is saturated, a significant NOE is observed on signal i (Figure 4A), suggesting that H_b and H_i are close

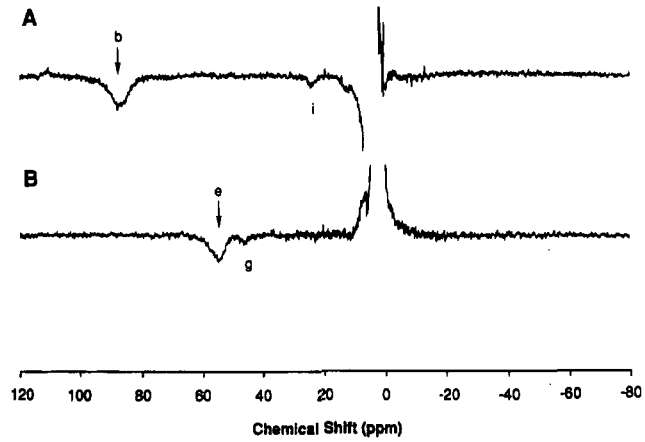

FIGURE 4: NOE difference spectra of Uf_r–WO_4 in H_2O buffer at 300 MHz and 30 °C in 100 mM acetate buffer at pH 4.9. The "super WEFT" technique was used to suppress the water signal. Irradiation signal and time: (A) signal b for 50 ms; (B) signal e for 50 ms.

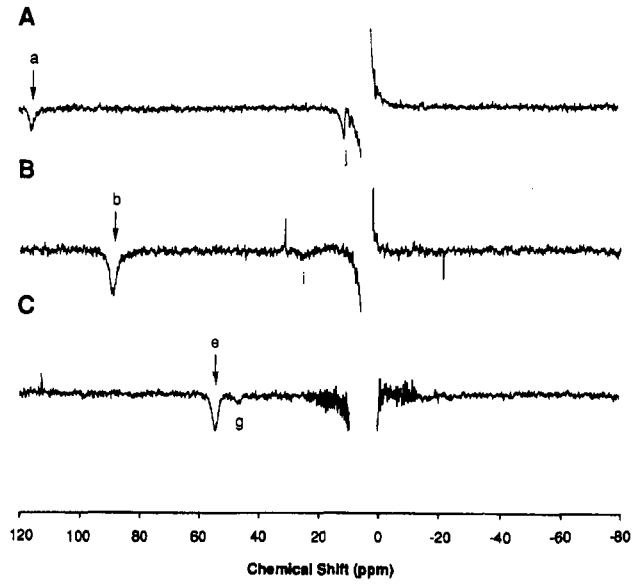

FIGURE 5: NOE difference spectra of $BSPAP_r$–WO_4 in H_2O buffer at 300 MHz and 30 °C in 100 mM acetate buffer at pH 4.9. The "super WEFT" technique was used to suppress the water signal. Irradiation signal and time: (A) signal a for 60 ms; (B) signal b for 50 ms; (C) signal e for 50 ms.

to each other. From its chemical shift and T_1 value, H_b is assigned to the N–H proton of the imidazole ring of the Fe(III)-coordinated His. So H_i is either the C_δ–H on an N_δ-coordinated His or one of the two geminal protons on the β-CH_2 group of a N_ϵ-coordinated His. However the chemical shift of H_i is inconsistent with that expected for the C_δ–H on an N_δ-coordinated His (~70 ppm) to an Fe(III) site (Scarrow et al., 1990), thus favoring the latter assignment. This implies that this His residue is N_ϵ-coordinated to the Fe(III) site. The signal due to the other geminal β-CH_2 proton that is expected if this assignment is correct could not be identified by irradiation of H_i and is presumably buried among the bulk protein resonances.

When signal e is saturated, a significant NOE on signal g is observed (Figure 4B), indicating that H_e and H_g are in close proximity of each other. H_e is the imidazole N–H proton of the Fe(II)-coordinated His residue based on its solvent exchangeability and chemical shift. H_g exhibits a chemical shift of 44.2 ppm, which is expected for the C_δ-H on an N_δ-coordinated His to an Fe(II) site (Scarrow et al., 1990). Thus the His on Fe(II) is N_δ-coordinated, with signals e and g corre-

sponding to the N_ϵ–H and C_δ–H protons, respectively.

Parallel NOE studies were carried on $BSPAP_r$–WO_4 instead of $BSPAP_r$ itself, because of the better resolution of the signals. When the 115.8 ppm signal (corresponding to signal a for Uf_r) is saturated (60 ms), a significant NOE on a signal at 12.0 ppm is observed (Figure 5A). This 12.0 ppm signal corresponds to signal j in Uf_r case. NOE studies on the two water-exchangeable signals at 89.2 and 54.5 ppm of $BSPAP_r$–WO_4 afford the same results as those from Uf_r–WO_4 studies. Significant NOE correlations between the 89.2 and 25.1 ppm signals (signals b and i, respectively) and between the 54.5 and 47.0 ppm signals (signals e and g, respectively) are observed (Figure 5B,C). These results support the conclusion that the diiron center of $BSPAP_r$–WO_4 has almost the same structure as that of Uf_r–WO_4. It also corroborates the assignments we made on the basis of our Uf NOE studies. However, unlike the Uf_r–WO_4 case, signal f appears farther upfield than signal g in the $BSPAP_r$–WO_4 spectrum! Thus the diiron active sites of Uf and BSPAP are quite similar but not identical.

Discussion

Our proton NMR studies demonstrate that reduced BSPAP exhibits well-resolved paramagnetically shifted ^1H NMR signals which correspond to signals found in the spectrum of reduced Uf. The spectral similarities are even more striking when the tungstate complexes are compared. On the basis of the above ^1H NMR observations, we conclude that the types of ligands, coordination number, and coordination geometry associated with the diiron active site of BSPAP are the same as those of Uf. However, the chemical shifts of corresponding signals and the integrations of one signal (signal i) from BSPAP and Uf are not identical, suggesting that small differences in the local coordination environments between the diiron active sites of these two proteins exist. It is unclear what protons correspond to the added intensity of signal i in the $BSPAP_r$ spectrum.

The NMR spectra of native Uf_r and $BSPAP_r$ differ in one important respect; while most of the corresponding signals are found within 5 ppm of each other, the shifts of proton a (Table I) which are assigned to one of the β-CH_2 protons of the coordinated tyrosine differ by 17 ppm. The fact that the shifts of the tyrosine C_δ–H protons (c, d) are nearly the same in the two proteins suggests that the extent of unpaired spin density delocalized by the ligand-to-metal charge-transfer transition is comparable in the two proteins and does not account for the different shifts of proton a. The shift of proton a is in part determined by the angle between the β–C–H bond and the p_π orbital on the C_γ carbon of the tyrosine (Scarrow et al., 1990). The β-CH_2 conformations relative to the Tyr aromatic ring must differ in the two enzymes and engender the chemical shift difference observed. Consistent with this notion, it has been proposed that differences in the conformation of the coordinated tyrosine residue may account for the different visible absorption maxima observed for the PAP's in their reduced states (510 nm for Uf and 536 nm for BSPAP) (Vincent et al., 1991b). The smaller difference in the absorption maxima of the two tungstate complexes (530 nm for Uf_r–WO_4 and 522 nm for $BSPAP_r$–WO_4) is also reflected by the closer similarity of their NMR spectra.

The NOE measurements performed on reduced Uf, Uf_r–WO_4, and $BSPAP_r$–WO_4 allow us to refine our earlier NMR assignments of the dinuclear iron center in Uf and to extend them to BSPAP as well. So far, all the downfield-shifted signals except signals f and h have been unambiguously assigned. The ligation of one tyrosine and one N_ϵ-coordinated histidine to Fe(III) and the ligation of one N_δ-coordinated histidine to Fe(II) are established. However, information about the remaining ligands has not been obtained, in part due to the limited number of the well-resolved NMR signals found in the spectra of the native proteins and their oxoanion complexes. The two remaining unassigned signals, i.e., signals f and h, may contain some information. Previous EXAFS studies found that the Fe–Fe separation in Uf and BSPAP is short (Que & Scarrow, 1988; Kauzlarich et al., 1986), suggesting that multiple bridging ligands between the two iron atoms are likely to be present. Model complex studies further demonstrated that, besides the single atom bridge, one additional carboxylate bridge is sufficient to limit the Fe–Fe distance to the small values found in these enzymes (Yan et al., 1988). Earlier, we suggested that signals f and g may arise from carboxymethylene protons of a coordinated Asp or Glu residue (Scarrow et al., 1990). Though our NOE results exclude signal g from being assigned to a carboxylate residue, our recent 1D and 2D NMR studies on $[Fe^{II}Zn^{II}(BPMP)(\mu\text{-}O_2CC_2H_5)_2]BPh_4$ [BPMP = 2,6-bis[[bis(2-pyridylmethyl)-amino]methyl]-4-methylphenol] show that chemical shift and relaxation time (T_1) values of the two CH_2 protons of the propionate bridges are close to those of signals f and h in the Uf and BSPAP cases (Z. Wang, T. R. Holman, and L. Que, Jr., unpublished results). As we did not see any NOE correlations between signal f and signal h, they do not arise from the same β-CH_2 group. Therefore, one of the two signals may come from one of the carboxymethylene protons of a bridging carboxylate ligand, while the other may arise from an Asp or Glu residue coordinated to the Fe(II) site. On the basis of the above results and suggestions, an updated model for the dinuclear iron centers of Uf and BSPAP is proposed (Figure 6). In order to observe more paramagnetically shifted resonances, and hence get more information about the other ligands, metal substitution at the Fe(II) site with metal ions with even shorter T_{1e} values should be very helpful. Such experiments are in progress (Haly et al., 1992).

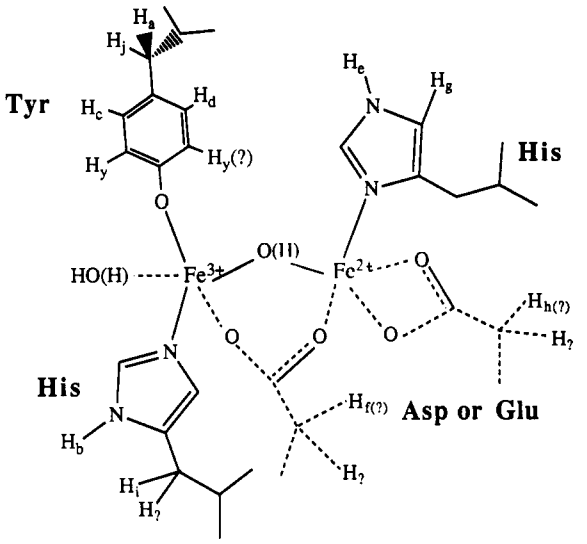

FIGURE 6: Updated model for the dinuclear iron center of mammalian PAP's. Ligands with dashed bonds to the diiron center have not been unequivocally established.

This work has demonstrated that the NOE technique is a powerful tool for identifying the connectivities among the ligand protons in an iron protein that contains neither a heme nor an iron–sulfur cluster. Such proteins typically exhibit isotropically shifted signals that are much broader than those found for heme proteins and iron–sulfur proteins. The fact that NOE's can be observed for such systems further enhances

the utility of NMR spectroscopy as a structural tool for metalloproteins.

References

Antanaitis, B. C., & Aisen, R. (1982) *J. Biol. Chem. 257*, 1855–1859.

Antanaitis, B. C., & Aisen, P. (1983) *Adv. Inorg. Biochem. 5*, 111–136.

Antanaitis, B. C., Aisen, P., Lilienthal, H. R., Roberts, R. M., & Bazer, F. W. (1980) *J. Biol. Chem. 255*, 11204–11209.

Antanaitis, B. C., Aisen, P., & Lilienthal, H. R. (1983) *J. Biol. Chem. 258*, 3166–3172.

Averill, B. A., Davis, J. C., Burman, S., Zirino, T., Sanders-Loehr, J., Loehr, T. M., Sage, J. T., & Debrunner, P. G. (1987) *J. Am. Chem. Soc. 109*, 3760–3767.

Basha, S. M., Bazer, F. W., Geisert, R. D., & Roberts, R. M. (1980) *J. Anim. Sci. 50*, 113–123.

Bertini, I., & Luchinat, C. (1986) *NMR of Paramagnetic Molecules in Biological Systems*, Benjamin/Cummings, Menlo Park, CA.

Campbell, H. D., Dionysius, D. A., Keough, D. T., Wilson, B. F., de Jersey, J., & Zerner, B. (1978) *Biochem. Biophys. Res. Commun. 82*, 615–620.

Davis, J. C., & Averill, B. A. (1982) *Proc. Natl. Acad. Sci. U.S.A. 79*, 4623–4627.

Day, E. P., David, S. S., Peterson, J., Dunham, W. R., Bonvoisin, J. J., Sands, R. H., & Que, L., Jr. (1988) *J. Biol. Chem. 263*, 15561–15567.

Dietrich, M., Münstermann, D., Suerbaum, H., & Witzel, H. (1991) *Eur. J. Biochem. 199*, 105–113.

Doi, K., Antanaitis, B. C., & Aisen, P. (1988) *Struct. Bonding (Berlin) 70*, 1–26.

Gaber, B. P., Sheridan, J. P., Bazer, F. W., & Roberts, R. M. (1979) *J. Biol. Chem. 264*, 8340–8342.

Haly, R. C., Que, L., Jr., & Ming, L.-J. (1992) *J. Am. Chem. Soc.* (in press).

Hochmann, J., & Kellerhals, H. (1980) *J. Magn. Reson. 38*, 23–29.

Hunt, D. F., Yates, J. R., III, Shabanowitz, J., Zhu, N.-Z., Zirino, T., Averill, B. A., Daurat-Larroque, S. T., Shewale, J. G., Roberts, R. M., & Brew, K. (1987) *Biochem. Biophys. Res. Commun, 144*, 1154–1160.

Inubushi, T., & Becker, E. D. (1983) *J. Magn. Reson. 51*, 128–133.

Kauzlarich, S. M., Teo, B. K., Zirino, T., Burman, S., Davis, J. C., & Averill, B. A. (1986) *Inorg. Chem. 25*, 2781–2785.

Ketcham, C. M., Roberts, R. M., Simmen, R. C. M., & Nick, H. S. (1989) *J. Biol. Chem. 264*, 557–563.

Lauffer, R. B., Antanaitis, B. C., Aisen, P., & Que, L., Jr. (1983) *J. Biol. Chem. 258*, 14212–14218.

Mockler, G. M., de Jersey, J., Zerner, B., O'Connor, C. J., & Sinn, E. (1983) *J. Am. Chem. Soc. 105*, 1890–1893.

Pyrz, J. W., Sage., J. T., Debruner, P. G., & Que, L., Jr. (1986) *J. Biol. Chem. 261*, 11015–11020.

Que, L., Jr., & Scarrow, R. C. (1988) *ACS Symp. Ser. 372*, 152–178.

Que, L., Jr., & True, A. E. (1990) *Prog. Inorg. Chem. 38*, 97–200.

Scarrow, R. C., Pyrz, J. W., & Que, L., Jr. (1990) *J. Am. Chem. Soc. 112*, 657–665.

Schlosnagle, D. C., Sander, E. G., Bazer, F. W., & Roberts, R. M. (1976) *J. Biol. Chem. 251*, 4680–4685.

Sinn, E., O'Connor, C. J., de Jersey, J., & Zerner, B. (1983) *Inorg. Chim. Acta 78*, L13–L15.

Vincent, J. B., & Averill, B. A. (1990) *FASEB J. 4*, 3009–3014.

Vincent, J. B., Crowder, M. W., & Averill, B. A. (1991a) *J. Biol. Chem. 266*, 11737–11740.

Vincent, J. B., Crowder, M. W., & Averill, B. A. (1991b) *Biochemistry 30*, 3025–3034.

Yan, S., Que, L., Jr., Taylor, L. F., & Anderson, O. P. (1988) *J. Am. Chem. Soc. 110*, 5222–5224.